Adsorption and Electrooxidation of DNA at Glassy Carbon Electrodes Modified with Multiwall Carbon Nanotubes Dispersed in Glucose Oxidase

Fabiana Gutierrez, María D. Rubianes, Gustavo A. Rivas**

INFIQC. Departamento de Físico Química. Facultad de Ciencias Químicas. Universidad Nacional de Córdoba. Ciudad Universitaria. 5000 Córdoba. Argentina
phone: +54-351-4334169/80; fax: +54-351-4334188.
*e-mail: grivas@mail.fcq.unc.edu.ar; rubianes@fcq.unc.edu.ar

Received: October 15, 2012
Accepted: November 14, 2012
Published online: ■■ ■■, 0000

Abstract
We are proposing for the first time the successful immobilization of DNA at glassy carbon electrodes (GCE) modified with carbon nanotubes (CNT) dispersed in glucose oxidase (GOx) (GCE/CNT-GOx) either by direct adsorption or by layer-by-layer self-assembling using polydiallyldimethylamine (PDDA). The presence of GOx allows an efficient dispersion of CNT and gives a most favorable environment that promotes the adsorption and makes possible a more sensitive electrooxidation of DNA. The PDDA incorporated in the self-assembled architecture largely facilitates the adsorption and electrooxidation of dsDNA and the adsorbed layer can be successfully used for evaluating the interaction of DNA with methylene blue.

Keywords: Carbon nanotubes dispersion, Double stranded calf-thymus DNA, Glucose oxidase, Self-assembling multilayers, Glassy carbon electrode, DNA-drug interaction, Methylene blue

DOI: 10.1002/elan.201200559

1 Introduction

Carbon nanomaterials have revolutionized not only the field of material sciences but also the area of biosensors due to their unique physical and chemical properties, their biocompatibility and robustness [1–3]. Particularly, since 1996, the use of carbon nanotubes (CNT) have allowed the development of electrochemical genosensors, immunosensors and enzymatic sensors with excellent analytical performance associated with high sensitivities, low detection limits, and fast responses [4–7].

It is important to remark that CNT tend to aggregate in aqueous solutions due to the strong interactions between their aromatic rings, making difficult their solubilization in usual solvents [8,9]. To overcome their aggregation and take profit of their full capabilities, CNT have been generally dispersed by non-covalent functionalization, since it makes possible a successful derivatization without disturbing their electronic characteristics [10–12]. In general, the functionalization involves the use of surfactants [13,14], biomolecules [15,16] and polymers [17–19], which not only disperse the CNT but also gives to the nanostructures particular characteristics depending on their inherent properties. Recently [20], we have reported the successful use of GOx as an excellent dispersing agent of CNT. The GCE modified with the resulting dispersion (GCE/CNT-GOx) have made possible a very efficient glucose biosensing, demonstrating that despite the drastic treatment during the preparation of the dispersion, GOx maintains their biorecognition properties [20].

In this work we evaluate the use of GCE modified with CNT-GOx as platform for DNA immobilization either by direct adsorption or by self-assembling of multilayers using the polycation polydiallyldimethylamine (PDDA) to connect the different layers.

The detection of DNA is an area of enormous interest in clinical, forensic, pharmaceutical and environmental sciences. Since early '90s, the design of DNA-based biosensors has been one of the important challenges in the field of biosensors due to the excellent recognition properties of DNA [21–23]. In fact, the recognition properties of DNA-modified electrodes has been explored in recent years using DNA fragments immobilized on surfaces modified with nanostructured thin films [24–26]. He and Bayachou [27] have proposed the immobilization of DNA on single-walled CNT (SWCNT) by layer-by-layer (L-B-L) deposition using PDDA as polycation. The resulting electrode has been used to evaluate the DNA damage in the presence of nitric oxide. Jin et al. [28] have reported the fabrication of multilayers films based on DNA/myoglobin on cysteamine-modified gold electrodes.

In the following sections we discuss the direct adsorption of double stranded calf-thymus DNA (dsDNA) and short oligonucleotides at GCE/CNT-GOx as well as the

influence of the experimental conditions on the adsorption of dsDNA and PDDA, the electrochemical characterization of the supramolecular architecture, and the interaction of the adsorbed DNA layer with methylene blue (MB).

2 Experimental

2.1 Apparatus

The measurements were performed with EPSILON (BAS) and TEQ_04 potentiostats. The electrodes were inserted into the cell (BAS, Model MF-1084) through holes in its Teflon cover. A platinum wire and Ag/AgCl, 3 M NaCl (BAS, Model RE-5B) were used as counter and reference electrodes, respectively. All potentials are referred to the latter. A magnetic stirrer provided the convective transport during the amperometric measurements. Electrochemical Impedance Spectroscopy (EIS) measurements were performed with a Solartron 1287 FRA 1260.

2.2 Reagents

Glucose oxidase (GOx) (Type X-S, *Aspergillus niger*, (EC 1.1.3.4), 50000 Units per gram of solid, Catalog number G-7141), double stranded calf-thymus DNA (dsDNA) (activated and lyophilized, catalog number D8899), single stranded calf-thymus DNA (ssDNA) and poly-diallyldimethylammonium chloride (PDDA) ($MW = 100000$–200000) were purchased from Sigma. The oligo$(dG)_7$ and oligo$(dG)_{11}$ and a random sequence of an oligodeoxynucleotide of 21 bases (oligo(dY), 3′ TAC ACC TTT TAG AGA TCG TCA 5′), were obtained from Life Technologies.

Methylene blue (MB) was purchased from Mallinckrodt. Potassium ferrocyanide and potassium ferricyanide were obtained from Merck. Multiwalled carbon nanotubes powder (CNT), (30 ± 15) nm diameter and 1–5 μ length, was obtained from NanoLab (USA). Other chemicals were reagent grade and used without further purification. Ultrapure water ($\rho = 18$ MΩ cm) from a Millipore-MilliQ system was used for preparing all the solutions.

2.3 Preparation of Glassy Carbon Electrodes Modified with CNTs

2.3.1 Preparation of the Dispersions

a) CNT-GOx: the dispersion was obtained by mixing 1.0 mg of CNT with 1.0 mL of 1.0 mg/mL GOx solution (prepared in 50 : 50 v/v ethanol/water) followed by sonication for 15 min.
b) CNT-Ethanol/water (CNT-Et): the dispersion was obtained by mixing 1.0 mg of CNTs with 1.0 mL of 50 : 50 v/v ethanol/water followed by sonication for 15 min.

2.3.2 Modification of Glassy Carbon Electrodes (GCE) with CNT-GOx (GCE/CNT-GOx) or CNT-Et/H_2O (GCE/CNT)

Previous to the modification, the GCEs were polished with alumina slurries of 1.0, 0.30, and 0.05 μm for 2 min each. The electrodes were then cycled between −0.300 V and 0.800 V at 0.050 V/s in a 0.100 M phosphate buffer solution pH 7.40 (10 cycles). After that, they were modified by dropping 20 μL of the CNT-GOx (or CNT-Et/H_2O) dispersion on the top of the surface followed by the evaporation of the solvent by exposure to air for 90 min.

2.4 Procedure

Cyclic voltammetry (CV) experiments were performed using 0.100 M phosphate buffer solution pH 7.40 or 0.020 M acetate buffer solution pH 5.00, while Linear Sweep Voltammetry (LSV) and Differential Pulse Voltammetry (DPV) experiments were performed in a 0.020 M acetate buffer solution pH 5.00. The analytical signals were obtained after subtracting the background currents.

EIS experiments were performed between 10 kHz and 10 MHz, with a potential perturbation of 0.010 V and a working potential of 0.200 V using 2.0×10^{-3} M potassium ferrocyanide and potassium ferricyanide as redox probe. The impedance spectra were analyzed by using the Z-view program.

2.5 Direct Adsorption and Adsorptive Voltammetric Stripping of DNA at GCE/CNT-GOx:

(I) *Pretreatment of the electrode:* the GCE, GCE/CNT-GOx and GCE/CNT were pretreated by cycling the potential (10 cycles) between −0.300 V and 0.800 V at 0.050 V/s in a 0.100 M phosphate buffer solution pH 7.40.
(II) *Adsorption of DNA:* pretreated GCE, GCE/CNT-GOx or GCE/CNT were immersed in a stirred 0.020 M acetate buffer solution pH 5.00 containing DNA for a given time at open circuit potential under stiring conditions.
(III) *Washing:* the electrodes were washed with a 0.020 M acetate buffer solution pH 5.00 for 10 s and then transferred to the stripping solution.
(IV) *Stripping:* it was performed by Linear Sweep Voltammetry (LSV) in a 0.020 M acetate buffer solution pH 5.00 between 0.500 V and 1.100 V at 0.050 V/s. The analytical signals were obtained after subtracting the background currents.

2.6 Layer-by-Layer Self-Assembly of DNA at GCE/CNT-GOx

(I) *Pretreatment of the electrode*: as indicated above.

(II) Adsorption of PDDA: it was performed at open circuit potential from a 3.0 mg/mL solution of PDDA (in a 0.050 M phosphate buffer solution pH 7.40) for 30.0 min.

(III) Washing: the electrodes were washed with a 0.020 M acetate buffer solution pH 5.00 for 10 s.

(IV) Adsorption of DNA: it was performed at open circuit potential from a 50.0 mg/mL solution of dsDNA in a 0.020 M acetate buffer solution pH 5.00 for 5.0 min.

(V) Washing: the electrodes were washed with a 0.020 M acetate buffer solution pH 5.00 for 10 s.

(VI) Stripping: it was performed by LSV in a 0.020 M acetate buffer solution pH 5.00 between 0.500 V and 1.100 V at 0.050 V/s. The analytical signals were obtained after subtracting the background currents.

2.7 DNA-MB Interaction at GCE/CNT-GOx/PDDA/dsDNA:

The protocol consisted of the following steps:

(*I*) to (V): as indicated above.

(VI) MB preconcentration: performed by immersion of GCE/CNT-GOx/PDDA/dsDNA in a 0.020 M acetate buffer solution pH 5.00 containing MB for a given time at open circuit potential under stirring conditions. Similar experiments were performed by using GCE/CNT-GOx and GCE/CNT-GOx/PDDA/ssDNA.

(VII) DPV-stripping: performed in a 0.020 M acetate buffer solution pH 5.00 by DPV between 0.300 and −0.500 V. DPV parameters: pulse height: 4 mV, scan rate: 20 mV s^{-1}, width: 50 ms and period: 200 ms, without stirring. The analytical signals were obtained after subtracting the background currents.

All the experiments were conducted at room temperature.

3 Results and Discussion

3.1 Direct Adsorption of dsDNA

Figure 1 shows voltammetric profiles obtained in a 0.020 M acetate buffer solution pH 5.00 at GCE (a), GCE/CNT (b) and GCE modified with CNT-GOx (c) after 20 min adsorption from 50.0 mg/L dsDNA. At GCE, under these experimental conditions, there is just a shoulder at around 0.800 V. At GCE/CNT (b) there is a peak at (0.603 ± 0.07) V due to guanine electrooxidation with an associated current that is 17 times larger than the one observed at bare GCE. At GCE/CNT-GOx (c) there is a well-defined peak at potentials more positive than at GCE/CNT (Peak potential, $E_p = 0.881 \pm 0.007$) V with an associated current (Peak current $i_p = 0.93 \pm 0.06$ μA) that is 31 and 1.8 times higher compared to bare GCE and GCE/CNT. Therefore, is clear that the presence of CNTs at GCE facilitates the adsorption of dsDNA and the electrooxidation of guanine residues due to their inherent catalytic activity. When GCE is modified with CNT-GOx, the negatively charged protein produces a shifting in the guanine electrooxidation signal to more positive potentials, although the oxidation current increases, probably due to a more efficient adsorption of the nucleic acid at a more biocompatible environment making possible a sensitive detection of dsDNA under conditions that at bare GCE it would be extremely difficult.

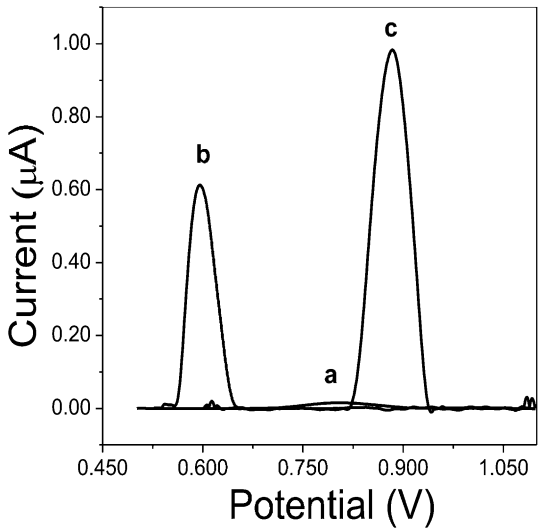

Fig. 1. Linear sweep voltammograms obtained in a 0.020 M acetate buffer solution pH 5.00 at (a) GCE, (b) GC/CNT and (c) GC/CNT-GOx after adsorption of 50.0 mg/L dsDNA. Experimental conditions: adsorption time: 20.0 min, adsorption potential: open circuit potential; scan rate: 0.050 V/s.

Figure 2 A shows the effect of the accumulation time of 100.0 mg/L dsDNA at GCE/CNT-GOx on the guanine oxidation currents obtained from cyclic voltammograms performed in a 0.020 M acetate buffer solution pH 5.00 at 0.050 V s^{-1} after medium exchange. The currents increase almost linearly with time up to 20 min, to level off thereafter. Therefore, 20 min was selected as the adsorption time. Figure 2 B shows the voltammetric profiles obtained in the acetate buffer solution after 20 min accumulation of different dsDNA solutions from 5.0 to 100.0 mg/L. A well-defined response is observed in all cases. The calibration plot (not shown) presents a linear range from 5.0 to 70.0 mg/L, a sensitivity of (0.016 ± 0.001) μA mg^{-1} L, a detection limit of 1.7 mg/L (obtained as $3.3\sigma/S$, where σ is the standard deviation of the blank signal and S the slope of the calibration plot), and a quantification limit of 5.6 mg/L (taken as $10\sigma/S$). The *RSD* obtained for the determination of 50.0 mg/L dsDNA with 12 electrodes and 4 different CNT-GOx dispersions was 6.0 %, indicating that the overall protocol from the preparation of the dispersion to the development of the sensor is highly reproducible.

The adsorption of short oligonucleotides at GCE/CNT-GOx was also evaluated. Figure 2 C displays the voltammetric behavior of GCE/CNT-GOx in acetate buffer solu-

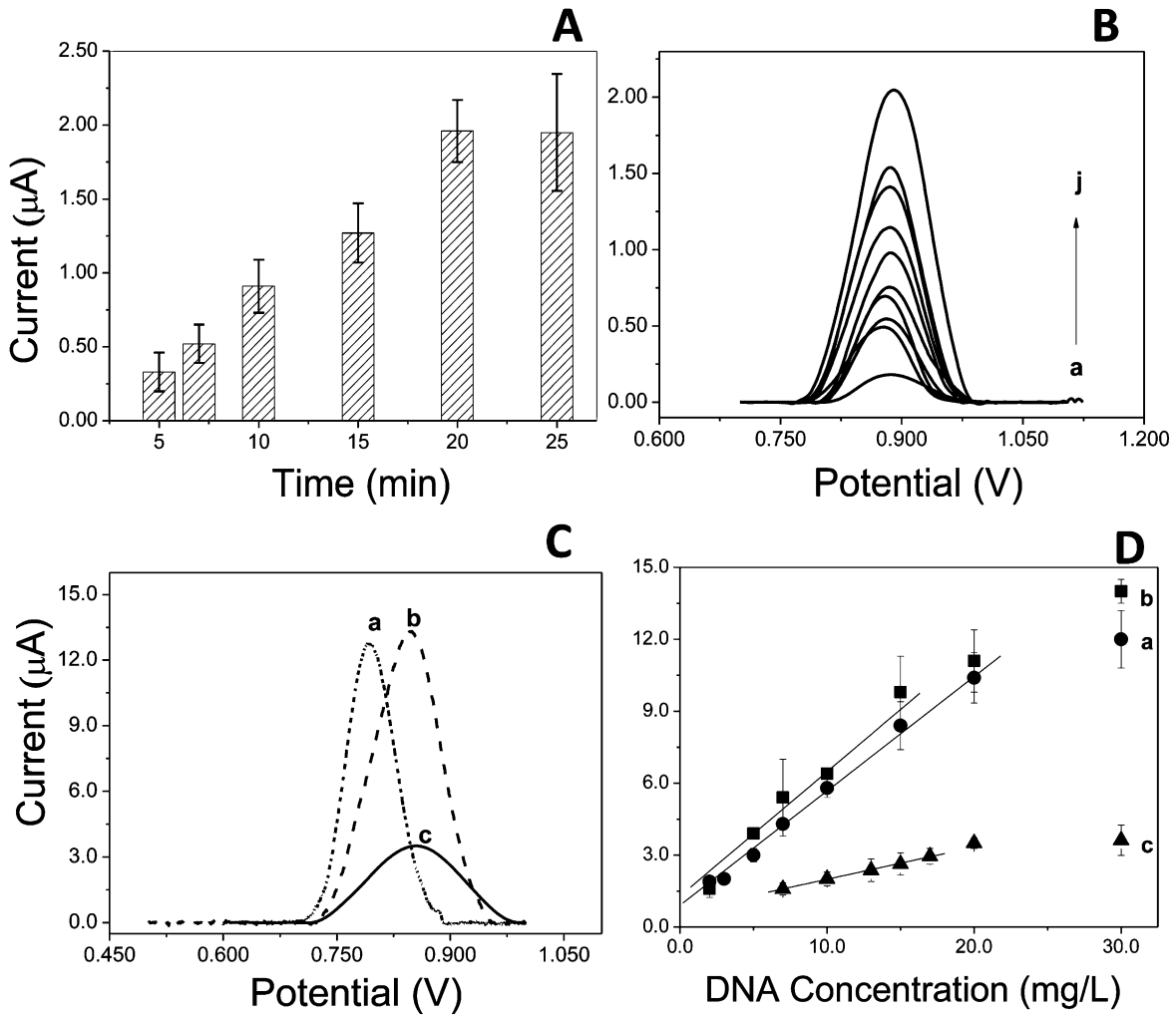

Fig. 2. A) Effect of the accumulation time in a 100.0 mg/L dsDNA on the guanine oxidation currents obtained after medium exchange from Linear sweep voltammograms in 0.020 M acetate buffer solution pH 5.00 at GCE/CNT-GOx at 0.050 $V s^{-1}$. B) Linear sweep voltammograms obtained at GC/CNT-GOx after adsorption of different concentrations of dsDNA for 5.0 min: a) 5.0 b) 20.0 c) 40.0, d) 60.0, e) 80.0, f) 100.0 mg/L. C) Linear sweep voltammograms obtained at GC/CNT-GOx after adsorption of 20.0 mg/L oligo$(dG)_7$ (a), oligo$(dG)_{11}$(b) (for 7 min) and 20.0 mg/L (oligo(dY) (c) (for 15 min). D) Calibrations plots obtained from Linear sweep voltammograms experiments at GC/CNT-GOx after adsorption of differents concentrations of oligo$(dG)_7$ (a), oligo$(dG)_{11}$(b) (for 7 min) and (oligo(dY) (c) (for 15 min). Other conditions as in Figure 1.

tion pH 5.00 after adsorption at open circuit potential of 20.0 mg/L oligo$(dG)_7$ (Figure 2C, a) and oligo$(dG)_{11}$(Figure 2C,b) for 7.0 min and 20.0 mg/L (oligo(dY) (Figure 2C,c) for 15.0 min. The oxidation currents for oligo$(dG)_7$ and oligo$(dG)_{11}$ are similar and considerably higher than that for oligo(dY). In fact, the sensitivities, obtained from the corresponding calibration plots showed in Figure 2D are (0.48 ± 0.03), (0.52 ± 0.03), and (0.13 ± 0.04) $\mu A\, mg^{-1} L$ for oligo$(dG)_7$, oligo$(dG)_{11}$ and oligo(-dY), respectively. These results suggest that the electrooxidation signal of the oligonucleotides depends on both, the trend to increase with the increment in the number of guanine residues and the trend to decrease with the increase in the length of the oligonucleotide. Similar behavior was reported for other carbonaceous surfaces [21,29,30]. It is important to mention that the overvoltages for the oxidation of guanine residues slightly increase as the size of the oligonucleotide increases. The oxidation peak potential for oligo$(dG)_7$ is 0.79 V, and it increases up to 0.85 V for oligo(dY), potential that is similar to the one obtained for the oxidation of dsDNA (0.88 V).

Regarding the stability of the platform GCE/CNT-GOx/dsDNA, it is important to remark that after immersing for 30 and 60 min in a 0.020 M acetate buffer solution pH 5.00 under stirring conditions and voltammetric stripping after medium exchange, the guanine oxidation signals remains statistically constant, decreasing just 1.5 and 3.7% of the original values, respectively.

3.2 Layer-by-Layer Self-Assembling of dsDNA at GCE/CNT-GOx

Considering the excellent results obtained by L-b-L self-assembling of polyelectrolytes in the construction of

(bio)sensors [31–35] and taking into account that GOx presents a negative charge under the working conditions, we evaluate the effect of the incorporation of a polycationic layer on GCE/CNT-GOx, previous to the adsorption of dsDNA, on the adsorption and electro-oxidation of dsDNA. The building of the multilayers system started with the adsorption of PDDA, followed by the adsorption of dsDNA. The additional layers were obtained by alternate adsorption of PDDA and dsDNA. After a careful evaluation of the adsorption conditions for PDDA and dsDNA, we selected 30 min adsorption of 3.0 mg/mL PDDA and 5.0 min adsorption for 50.0 mg/L dsDNA as optima conditions.

Table 1 shows the peak currents and peak potentials for the electrooxidation of guanine obtained from LSV profiles for electrodes containing one, two and tree bilayers of PDDA/dsDNA (GCE/CNT-GOx/(PDDA/dsDNA)$_n$, where n = number of PDDA/dsDNA bilayers). The guanine oxidation current for the electrode with one PDDA/dsDNA bilayer was significantly higher (7.6 times) than the one obtained at GCE/CNT-GOx while the peak potential was 181 mV smaller. These results demonstrate that the presence of the polycation clearly facilitates the adsorption of dsDNA, (promoted by electrostatic interaction) and the charge transfer. When a new bilayer of PDDA/dsDNA is incorporated, (GCE/MWNT-GOx/(PDDA/dsADN)$_2$) the signal for DNA oxidation appeared at a potential almost the same as the one for GC/MWNT-GOx/PDDA/dsADN, while the current increased 3.4 times ((24 ± 5) μA vs. (7 ± 2) μA for $n=2$ and $n=1$, respectively). Therefore, is clear that the incorporation of a second layer of PDDA facilitates the adsorption of a new layer of DNA. Further adsorption of PDDA and dsDNA (GC/CNT-GOx/[PDDA/dsADN]$_3$), does not produce significant changes in current ($i_p=28\pm5$) μA. This effect was attributed to a less effective charge reversion when building the supramolecular architectures.

The calibration plot obtained for dsDNA at GCE/CNT-GOx/PDDA after 5.0 min adsorption showed a linear range between 5.0 and 60.0 mg/L with a sensitivity of (0.15 ± 0.02) μA mg/L, a detection limit of 600 μg/L and a quantification limit of 2.0 mg/L (calculated as it was previously indicated). The response was highly reproducible since the *RSD* obtained for the determination of 20.0 mg/L dsDNA with 9 electrodes and 3 dispersions was 3.0 %.

The supramolecular architecture was also characterized by EIS using 2.0×10^{-3} M $Fe(CN)_6^{-3/-4}$ as redox markers (in a 0.10 M phosphate buffer solution pH 7.40). The evaluation of the system was performed using a Randles circuit. Figure 3 depicts the normalized charge transfer resistance (R_N) obtained at GCE/CNT-GOx after the adsorption of alternate layers of PDDA and dsDNA. R_N is the ratio between the R_{ct} of each layer and the R_{ct} for GCE/CNT-GOx ($R_N=R_{ct}/R_{ct(GCE/CNT\text{-}GOx)}$) obtained from Nyquist plots. The inset displays the Nyquist plots obtained for the redox probe at GCE/CNT-GOx (a), GCE/CNT-GOx/PDDA (b) and GCE/CNT-GOx/PDDA/dsDNA (c). In all cases, there is a typical resistive component at high frequencies and a diffusional one at lower frequencies. When PDDA is adsorbed for 30 min at GCE/CNT-GOx, the R_N decreases around 40 % ((1.0 ± 0.08) vs. (0.6 ± 0.1)), demonstrating that the presence of the positively charged layer facilitates the charge transfer of the probe due to the screening of the negative charges of CNT-GOx. When 50.0 mg/L dsDNA is adsorbed for 5.0 min at GCE/CNT-GOx/PDDA the R_N slightly increases due to the electrostatic repulsion between the negatively charged marker and the negatively charged phosphate backbone. The incorporation of a second layer of PDDA produces a new decrease in R_N indicating the successful adsorption of the polycation and the facilitated charge transfer of the redox probe. The adsorption of a second layer of dsDNA produces a new increase in the R_N. Further adsorption of PDDA and dsDNA, does not produce significant changes in R_N, in agreement with the voltammetric results previously discussed.

The platform GCE/CNT-GOx/PDDA/dsDNA demonstrated to be highly stable since after 60 min immersion in a 0.020 M acetate buffer solution pH 5.00 under stirring conditions and voltammetric stripping after medium exchange, the guanine oxidation signals remains in a 100 % of the original value.

Table 1. Peak currents for the electrooxidation of guanine obtained from LSV profiles for electrodes containing 1, 2 and 3 bilayers of PDDA/dsDNA.

	Current (μA)	Potential (V)
GC/CNT-GOx/PDDA/dsADN	7 ± 2	0.70 ± 0.01
GC/CNT-GOx[PDDA/dsADN]$_2$	24 ± 5	0.69 ± 0.01
GC/CNT-GOx[PDDA/dsADN]$_3$	28 ± 5	0.66 ± 0.01

3.3 Interaction of GCE/CNT-GOx/PDDA/dsDNA with Methylene Blue

The capability of the adsorbed dsDNA layer to interact with intercalators was evaluated by studying the interaction of dsDNA immobilized at GCE/CNT-GOx/PDDA with methylene blue (MB). MB is an organic dye that belongs to the phenothiazine family and it is a well-known hybridization indicator of DNA. MB interacts with guanine residues of DNA [36–40], and by intercalation [41,42].

Figure 4 shows the CVs obtained at GCE/CNT-GOx/PDDA/dsDNA in a 0.020 M acetate buffer solution pH 5.00 after interaction for 5.0 min at open circuit potential in acetate buffer solution (dotted line) and in a 2.0×10^{-5} M MB solution (solid line) previous medium exchange. The voltammogram obtained after 5.0 min in buffer solution, shows only the peaks system at around −0.40 V due to the reduction/oxidation of FAD/$FADH_2$ present at the electrode surface [20]. In the voltammogram obtained after MB accumulation, in addition to those peaks, there is another peaks system due to the re-

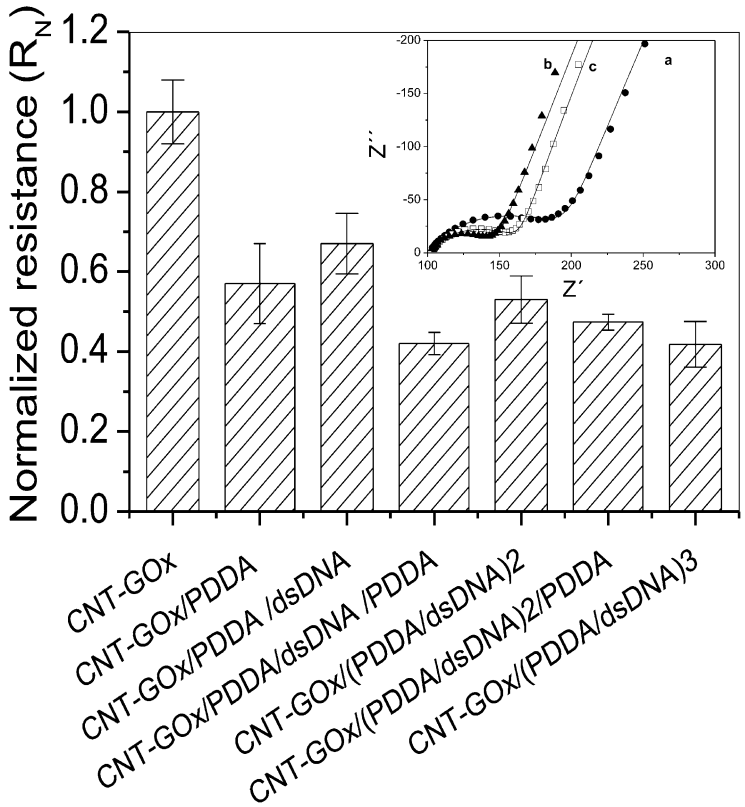

Fig. 3. Normalized charge transfer resistance (R_N) ($R_N = R_{ct}/R_{ct(GCE/CNT\text{-}GOx)}$) obtained from Nyquist plots for GCE/CNT-GOx after the adsorption of alternate layers of PDDA and dsDNA. Experimental conditions: concentration of dsDNA: 50.0 mg/L, adsorption time: 5.0 min; concentration of PDDA: 3.0 mg/mL, accumulation time: 30.0 min. Redox marker: $Fe(CN)_6^{-3/-4}$, supporting electrolyte: 0.100 M phosphate buffer pH 7.40. Inset: Nyquist plots obtained for GCE/CNT-GOx (a), GCE/CNT-GOx/PDDA (b) and GCE/CNT-GOx/PDDA/dsDNA (c).

duction of MB (at −0.23 V) and its reoxidation (at −0.13 V). Similar experiments without previous accumulation show almost no peak currents associated with the redox behavior of MB (see Inset).

Cyclic voltammograms obtained at bare GCE in a 0.020 M acetate buffer solution pH 5.00 after accumulation in a 2.0×10^{-5} M MB and medium exchange presented just a broad peak at around −0.35 V due to the reduction of the oxidized product of MB, although it is overlapped with the oxygen reduction (not shown). At GCE/CNT, there is a clear definition of the processes associated with the oxidation and reduction of MB. MB is oxidized at −0.16 V and the reduction occurs at −0.17 V. Cyclic voltammograms obtained at GCE/CNT-GOx/PDDA under identical experimental conditions, presented the two peaks previously discussed, associated with the couple FAD/$FADH_2$, and two additional ones at more positive values due to the oxidation ($E_p = -0.14$ V) and reduction ($E_p = -0.22$ V) of MB. The MB signals were around 30% higher than those obtained at GCE/CNT-GOx/PDDA/dsDNA due to the absence of the intercalation process.

The interaction of MB with GCE/CNT-GOx/PDDA modified with ssDNA instead of dsDNA was also evaluated. Figure 5A displays DPV profiles obtained in acetate buffer solution after adsorption of 2.0×10^{-5} M MB for 5.0 min at GCE/CNT-GOx (a), GCE/CNT-GOx/PDDA/ssDNA (b) and GCE/CNT-GOx/PDDA/dsDNA (c). The presence of DNA, either ss or dsDNA produces a decrease in the MB reduction signal due to the interaction with DNA, although this decrease is most important in the case of the double helix as a consequence of the intercalation of MB [35]. This system was also interrogated by EIS. Figure 5B shows the Nyquist plots using $Fe(CN)_6^{-3/-4}$ as redox marker in a 0.10 M phosphate buffer solution pH 7.40 at GCE/CNT-GOx/PDDA/ssADN (a) and GCE/CNT-GOx/PDDA/dsADN (b) after interaction with 2.0×10^{-5} M MB for 5.0 min. The system was evaluated using the Randles circuit. The charge transfer resistances obtained from the Nyquist plots before and after adsorption indicate that the R_{ct} decreases when MB is adsorbed. This facilitated charge transfer of the redox probe, confirms the immobilization of MB and the screening of the negative charges of dsDNA. When MB was accumulated on GCE/CNT-GOx/PDDA/dsDNA the R_{ct} was smaller than on GCE/CNT-GOx/PDDA/ssDNA ($(29.6\pm0.5)\ \Omega$ vs. $(46.03\pm0.09)\ \Omega$), in agreement with the voltammetric results, since at dsDNA MB interacts not only by electrostatic forces, but also by intercalation within he double helix [42].

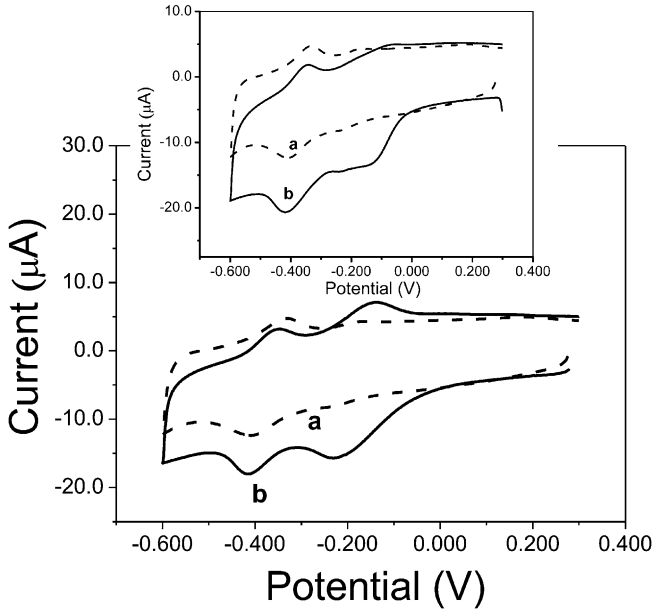

Fig. 4. Cyclic voltammograms obtained at GCE/CNT-GOx/PDDA/dsDNA in a 0.020 M acetate buffer solution pH 5.00 after 5.0 min accumulation in a 0.020 M acetate buffer solution pH 5.00 (a, dotted line), and after 5.0 min accumulation in a 2.0×10^{-5} M MB (b, solid line). Accumulation potential: open circuit. The inset shows cyclic voltammograms obtained without accumulation at GCE/CNT-GOx/PDDA/dsDNA in a 0.020 M acetate buffer solution pH 5.00 (a, dotted line) and in a 2.0×10^{-5} M MB solution (b, solid line). Scan rate: 0.010 V/s.

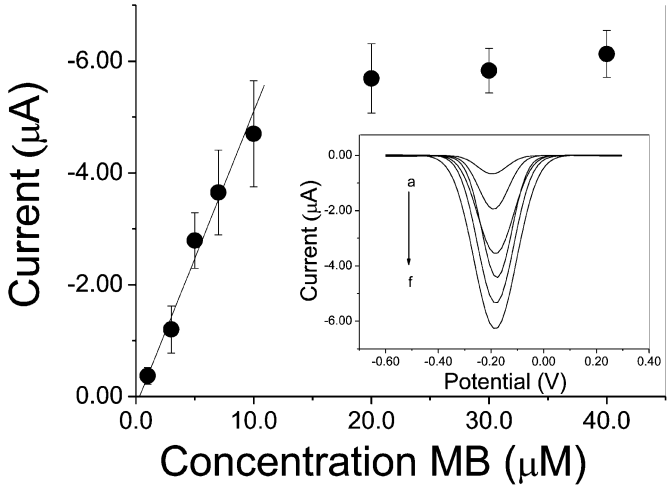

Fig. 6. Calibration plot obtained from DPV experiments at GCE/CNT-GOx/PDDA/dsDNA in a 0.020 M acetate buffer solution pH 5.00 after accumulation at open circuit potential in solutions of MB of different concentration. Inset: DPVs obtained at GCE/CNT-GOx/PDDA/dsDNA in a 0.020 M acetate buffer solution pH 5.00 after accumulation at open circuit potential in solutions of MB of different concentrations: a) 1.0 b) 3.0 c) 5.0 d) 10.0 e) 20.0 and f) 40.0 μM. Other conditions as in Figure 5 A.

Even when the main goal of this work was not the quantification of MB at GCE/CNT-GOx/dsDNA, is also important to mention that the platform is also useful for the submicromolar quantification of MB. Figure 6 shows the calibration plot for MB obtained after 5.0 min interaction with GCE/CNT-GOx/PDDA/dsDNA. The linear range goes from 1.0 to 10.0 μM, the sensitivity is (0.53 ± 0.07) μA μM^{-1}, the detection limit is 0.07 μM, and the quantification limit is 0.23 μM (calculated as it was previously indicated). The *RSD* for 20 μM MB was 7.0% for 7 electrodes and 3 different dispersions. The inset in Figure 6 shows the DPV profiles obtained after 5.0 min accumulation for different concentrations of MB from 1.0

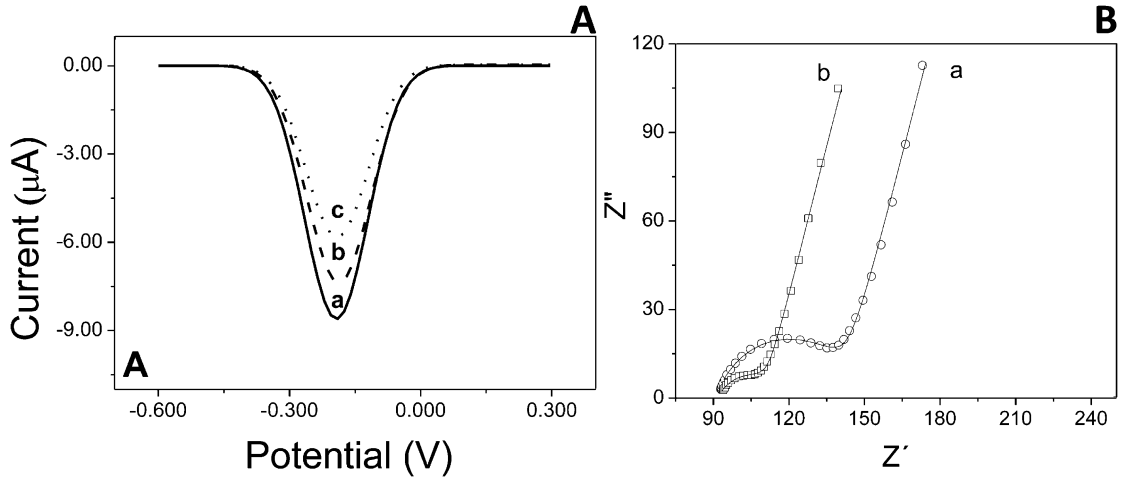

Fig. 5. A) Differential pulse voltammograms obtained at GCE/CNT-GOx (a) GCE/CNT-GOx/PDDA/ssDNA (b) and GCE/CNT-GOx/PDDA/dsDNA (c) in a 0.020 M acetate buffer solution pH 5.00 after accumulation at open circuit potential in a 2.0×10^{-5} M MB. Experimental conditions of DPV: potential range between 0.300 and −0.500 V: pulse height of 4mV, scan rate of 20mVs^{-1}, width of 50 ms and period of 200 ms, without stirring. The analytical signals were obtained after subtracting the background currents. B) Nyquist plots at GCE/CNT-GOx/PDDA/ssADN (a) and GCE/CNT-GOx/PDDA/dsADN (b) after the adsorption in MB. Experimental conditions: concentration of MB: 2.0×10^{-5} M, adsorption time: 5.0 min. Redox marker: $Fe(CN)_6^{-3/-4}$, supporting electrolyte: 0.100 M phosphate buffer pH 7.40.

to 40.0 μm. These profiles demonstrate that in all cases the response is clear and well-defined.

4 Conclusions

We are proposing for the first time the successful building of platforms based on the use of GCE/CNT-GOx and the immobilization of DNA as biorecognition element either by direct adsorption or by L-b-L self-assembling using PDDA as polycation. The presence of GOx allows the efficient dispersion of CNT and even most important, gives to the platform a most favorable and biocompatible environment that promotes the adsorption of DNA. The presence of PDDA in the self-assembled architecture largely facilitates the adsorption of the nucleic acid and the adsorbed layer can be successfully used for evaluating the interaction of DNA with MB, opening the doors to many important and new developments in the field of DNA-drug interactions and DNA damage.

Acknowledgements

The authors thank *CONICET*, *MINCyT-Córdoba*, *SECyT-UNC* and *ANPCyT* for the financial support. F. A. G. thanks *CONICET* for the fellowship.

References

[1] S. K. Vashist, D. Zheng, K. Al-Rubeaan, J. H. T. Luong, F.-S. Sheu, *Biotechnol. Adv.* **2011**, *29*, 169.
[2] A. Sassolas, L. J. Blum, B. D. Leca-Bouvier, *Biotechnol. Adv.* **2012**, *30*, 489.
[3] T. Premkumara, K. E. Geckelera, *Prog. Polymer Sci.* **2012**, *37*, 515.
[4] I. Willner, B. Willner, *Nano Lett.* **2010**, *10*, 3805.
[5] M. Tunckol, J. Durand, P. Serp, *Carbon* **2012**, *50*, 4303.
[6] B. Jacobs, M. J. Peairs, B. J. Venton, *Anal. Chim. Acta* **2010**, *662*, 105.
[7] P. Cheng Ma, N. Siddiqui, G. Marom, J. K. Kima, *Composites Part A* **2010**, *41*, 1345.
[8] G. Dreselhaus, M. A. Pimenta, R. Saito, J.-C. Charlier, S. D. M. Brown, P. Corio, A. Marucci, M. S. Dresselhaus, *Science and Applications of Nanotubes* (Eds: D. Tomanek, R. J. Enbody), Kluwer Academic, New York **2000**, pp. 275–295.
[9] M. F. Lin, D. S. Chuu, *Phys. Rev. B: Condens. Matter Mater. Phys.* **1998**, *57*, 10186.
[10] C. Gao, Z. Guo, J-H Liu, X-J. Huang, *Nanoscale* **2012**, *4*, 1948.
[11] L. Hu, D. S. Hecht, G. G. Grüner, *Chem. Rev.* **2010**, *110*, 5790.
[12] D. Tuncel, *Nanoscale* **2011**, *3*, 3545.
[13] V. Sanz, E. Borowiak, P. Lukanov, A. M. Galibert, E. Plahaut, H. M. Coley, S. Ravi, P. Silva, J. Mc Falden, *Carbon* **2011**, *49*, 1775.
[14] J. Rausch, R-Ch. Zhuang, E. Mäder, *Composites: Part A* **2010**, *41*, 1038.
[15] X. Wu, Z. Zhen, J. H. Jiang, G. L. Shen, R. Q. Yu, *J. Am. Chem. Soc.* **2009**, *31*, 12325.
[16] H. Yang, Y. Zhu, D. Chen, C. Li, S. Chen, Z. Ge, *Biosens. Bioelectron.* **2010**, *26*, 295.
[17] R. Olivé-Monllav, M. J. Esplandiú, M. J. Bartroli, M. Baeza, F. Céspedes, *Sens. Actuators B* **2010**, *146*, 353.
[18] N. G. Sahoo, S. Rana, J. W. Cho, L. Li, S. H. Chan, *Prog. Polymer Sci.* **2010**, *35*, 837.
[19] S. W. Kim, T. Kim, Y. S. Kim, H. S. Choi, H. J. Lim, S. J. Yang, C. R. Park, *Carbon* **2012**, *50*, 3.
[20] F. Gutierrez, M. D. Rubianes, G. A. Rivas, *Sens. Actuators B* **2012**, *161*, 191.
[21] E. Palecek, M. Bartosík, *Chem. Rev.* **2012**, *112*, 3427.
[22] J. Ezzati N. Dolatabadi, O. Mashinchian, B. Ayoubi, A. A. Jamali, A. Mobed, D. Losic, Y. Omidi, M. de la Guardia, *Trends Anal. Chem.* **2011**, *30*, 459.
[23] T. Premkumara, K. E. Geckelera, *Prog. Polymer Sci.* **2012**, *37*, 515.
[24] M. Das, G. Sumana, R. Nagarajan, B. D. Malhotra, *Thin Solid Films* **2010**, *519*, 1196.
[25] A. Walcarius, *Trends Anal. Chem.* **2012**, *38*, 79.
[26] S. Chatterjee, A. Chen, *Electrochem. Commun.* **2012**, *20*, 29.
[27] P. G. He, M. Bayachou, *Langmuir* **2005**, 21, 6086.
[28] Y. D. Jin, Y. Shao, S. J. Dong, *Langmuir* **2003**, *19*, 4771.
[29] X. Cai, G. Rivas, P. A. M. Farias, H. Shiraishi, J. Wang, E. Palecek, *Electroanalysis* **1996**, *8*, 753.
[30] M. L. Pedano, G. A. Rivas, *Biosens. Bioelectron.* **2003**, *18*, 269.
[31] G. Decher, *Science* **1997**, *29*, 1232.
[32] R. M. Lost, F. N. Crespilho, *Biosens. Bioelectron.* **2012**, *31*, 1.
[33] Y. Lvov, G. Decher, H. Mohwald, *Langmuir* **1993**, *9*, 481.
[34] A. J. Lin, Y. Wen, L. J. Zhang, B. Lu, Y. Li, Y. Z. Jiar, H. F. Yang, *Electrochim. Acta* **2011**, *56*, 1030.
[35] H. B. Shi, Y. Yang, J. D. Huang, Z. X. Zhao, X. H. Xu, J. I. Anzai, T. Osa, Q. Chen, *Talanta* **2006**, *70*, 852.
[36] A. Erdem, K. Kerman, B. Meric, M. Ozsoz, *Electroanalysis* **2001**, *13*, 219.
[37] D. Ozkan, P. Kara, K. Kerman, B. Meric, A. Erdem, F. Jelen, P. E. Nielsen, M. Ozsoz, *Bioelectrochemistry* **2002**, *58*, 119.
[38] W. Yang, M. Ozsoz, D. B. Hibbert, J. J. Gooding, *Electroanalysis* **2002**, *14*, 1299.
[39] R. Rohs, H. Sklenar, R. Lavery, B. Röder, *J. Am. Chem. Soc.* **2000**, *122*, 2860.
[40] M. Enescu, B. Levy, V. Gheorghe, *J. Phys. Chem. B* **2000**, *104*, 1073.
[41] S. O. Kelley, E. M. Boon, J. K. Barton, N. M. Jackson, M. G. Hill, *Nucl. Acids Res.* **1999**, *27*, 4830.
[42] A. Tani, A. J. Thomson, J. N. Butt, *Analyst* **2001**, *126*, 1756.

